HOOD: a Real Environment Human Odometry Dataset for Wearable Sensor Placement Analysis

Barbara Bruno, Fulvio Mastrogiovanni and Antonio Sgorbissa

***Abstract*— Human Odometry (HO) is the process of providing a person with a continuous estimate of their location, on the basis of information acquired solely by sensors carried around by the person themselves. In an effort towards the development of effective and robust HO systems, we present the Human Odometry Outdoor Dataset (HOOD), a public collection of labelled accelerometer and gyroscope data recordings. We compare four sensor placements (foot, waist, wrist, chest) to identify the most suitable placement for different types of motions (ranging from walking to slithering), occurring in highly diverse real environments (such as flat grass fields, staircases and rough terrains).**

I. Introduction

The U.S. Homeland Security Presidential Directive HSPD-8 defines First Responders as “individuals who in the *early stages of an incident* are responsible for the protection and preservation of life, property, evidence, and the environment, [...] that provide *immediate support* services during prevention, response, and recovery operations.” First Responders typically include policemen, fire-fighters and emergency medical responders, and the incidents they have to face range from urban hazards like traffic collisions and train wrecks to natural disasters such as wildfires, earthquakes and floods.

The unparalleled difficulty of First Responders missions arises from the fact that incidents usually cause unpredictable changes in the environment, significantly affecting the way humans can act in it: for example, floors of a building that are normally accessible by staircases and elevators could become inaccessible due to an earthquake. For individuals having to provide *immediate support* in the *early stages of an incident* this translates to finding themselves in an unknown and dangerous environment, with no time to explore it.

Under these conditions, one crucial factor for the success of First Responders missions is the possibility for team members to always know their position and the path to follow to get out of the dangerous zone. Moreover, the knowledge of first responders location is a key requirement for robots that have to cooperate with them in disaster scenarios [1]. The task of providing a person with a continuous estimate of their location, on the basis of information acquired by sensors carried around by the person themselves, is called Human Odometry, or Personal Dead Reckoning (PDR) [2].

In the Literature about Human Odometry, this task (which is typically faced in mobile robotics through the integration of wheel encoder readings) is divided in two sub-problems:

B. Bruno, F. Mastrogiovanni and A. Sgorbissa are with the Department of Informatics, Bioengineering, Robotics and Systems Engineering, University of Genova, Via Opera Pia 13, 16145 Genova, Italy.
Corresponding author’s email: barbara.bruno@unige.it.

(a) Slow walk (b) Normal walk (c) Run
(d) Slow crawl (e) Fast crawl (f) Slither

Fig. 1. The 6 motion types considered in HOOD. By considering the orientation of the torso with respect to gravity, we define (a) *slow walk*, (b) *normal walk* and (c) *run* as vertical-stance activities, and (d) *slow crawl*, (e) *fast crawl* and (f) *slither* as horizontal-stance activities.

- to estimate the travelled distance,
- to track the heading of the person.

Albeit all based on accelerometer data, various techniques have been envisaged and adapted to estimate the travelled distance: the simplest but less accurate systems rely on step detection algorithms with fixed step length [2], while similar but more accurate solutions train neural networks to properly estimate the step length [3]. Recent approaches implement the Extended Kalman Filter and the Zero Velocity Update strategy to reduce the inertial measurements drift [4]. Heading tracking can be based on gyroscope data exclusively [5], [6] or gyroscope and compass data [7], [4]. Commonly adopted techniques for the reduction of the heading drift range from periodic resets based on GPS information [8], to systematic corrections obtained by analysing street segments in a database of street maps [9]. Other methods make use of environmental tags previously deployed in the building [4], while the most complex cooperative positioning systems rely on sharing information among multiple nodes [7].

Surprisingly enough, the majority of existing HO systems in the Literature are centred on two assumptions, which greatly limit the possibility of using them in real missions: (i) few systems consider more than the single walking motion (extended studies usually add slopes and stairs [6], [10]) and there are no comprehensive analyses of the performance of HO systems with respect to different motions; (ii) few systems consider other than a foot placement for the sensing device (among them, systems relying on the sensory capabilities of smartphone usually either adopt a waist place-

Preprint submitted to 2015 IEEE/RSJ International Conference on Intelligent Robots and Systems. Received March 4, 2015.

(a) Grass field (b) Uphill road (c) Staircase

(d) River bed (e) Woods (f) Snow

Fig. 2. The 6 outdoor environments considered in HOOD. The motions *slow walk*, *normal walk* and *run* were performed in all environments, while the motions *slow crawl*, *fast crawl* and *slither* were executed in the grass field environment only. The test environments include three scenarios with even ground: (a) a flat *grass field* (football field), (b) an *uphill asphalt road* (with a constant slope of about 25%) and (c) a wide *staircase*; and three scenarios with rough terrain: (d) a rocky *river bed*, (e) a bumpy *woods* hill and (f) a field covered in snow.

ment [11], or make use of hand-held or shoulder-mounted devices [2]) and there are no comprehensive analyses of the performance of HO systems with respect to different sensor placements. Furthermore, there are no systematic studies on the performance of HO systems under highly diverse conditions. Indeed, developing reliable HO systems that retain good accuracy even when the person is walking in rough terrains, such as snow or in the woods, crawling or slithering, is a fundamental step towards their deployment in real conditions. Consequently, it is also necessary to gather representative datasets and make them publicly available, to allow comparisons between different approaches.

The contribution of the article is three fold: (i) an analysis of diverse outdoor environments, to define the challenges they present to wearable systems for Human Odometry; (ii) an analysis of the characteristics of different motion types, to identify the requirements they pose on the HO system for accurate path reconstruction; (iii) a comparison of the accuracy of a standard step counting algorithm across different environments and motion types, to identify the most suitable sensor placements. All reported analyses are performed over a dataset that considers 6 real environments (staircases, flat grass field, uphill road, flat rough terrain - river bed, uphill rough terrain - woods, snow), 6 motion types (slow walking, normal walking, running, slow crawling, fast crawling, slithering) and 4 sensor placements (foot, waist, wrist, chest), which we have made publicly available.

The article is organized as follows: Section II introduces HOOD, the public dataset that we have collected, and Section III defines the applied step detection procedure. Section IV reports considerations about the most suitable sensor placement as a function of the ground conditions in the test environment, while Section V analyses the step detection accuracy associated with the different sensor placements with respect to the performed motion. Conclusions follow.

II. Human Odometry Outdoor Dataset

We present HOOD (Human Odometry Outdoor Dataset), a public dataset[1] for the evaluation of HO systems based on accelerometer and gyroscope data. The dataset is composed of 168 trials, referring to the combinations of the six motion types shown in Figure 1, the six outdoor environments shown in Figure 2 and the four device placements shown in Figure 3, once tested with the person walking along a straight line and once with the person walking along a zig-zag path, i.e., alternatively taking left and right turns. Each trial records the 6DOF acceleration and angular rate values registered during one execution of one combination and is annotated with the number of steps effectively taken.

Hardware specifications. In all recordings we used a small ad-hoc sensing device equipped with the commercial 6DOF Inertial Measurement Unit (IMU) InvenSense MPU6050. The accelerometer is set to have a measurement range of $[-2g;+2g]$ with a sensitivity of 16 bits per axis. The gyroscope is set to have a measurement range of $[-250;+250]$ with a sensitivity of 131 LSBs/dps. The sampling frequency is 40 Hz for both sensors. The 4 different placements and orientations of the device are shown in Figure 3.

Acquisition procedure. All the trials were recorded in a series of supervised experiments, in the scenarios shown in Figure 2. In the *grass field* environment, all 48 combinations of 6 motion types, 4 sensor placements and 2 path configurations were tested. For obvious feasibility reasons, in all other environments we considered vertical-stance activities

[1]The dataset and its detailed description are freely available at: http://github.com/fulviomas/HOOD

Preprint submitted to 2015 IEEE/RSJ International Conference on Intelligent Robots and Systems. Received March 4, 2015.

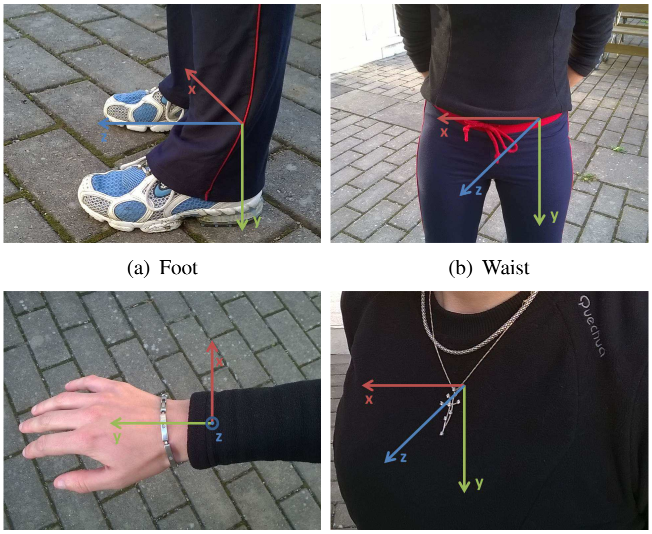

(a) Foot (b) Waist (c) Wrist (d) Chest

Fig. 3. The 4 sensor placements considered in HOOD.

only (i.e., the motions *slow walk*, *normal walk* and *run*), therefore testing the 120 combinations originated by the 5 environments, 3 vertical-stance motions, 4 sensor placements and 2 path configurations. During the tests, given the list of all different combinations, a volunteer equipped with the device is asked to perform one specific combination, to which the supervisor associates the corresponding IMU data and the number of taken steps (knee or elbow hits in case of crawling and slithering motions, respectively).

Dataset description. We argue that First Responders missions in outdoor environments usually take place in one of the six scenarios shown in Figure 2. More generally, HOOD datasets provides examples of: *flat* (grass field, river bed, snow), or *sloping* (uphill road, staircase, woods) terrains, with *even* (grass field, uphill road, staircase), *bumpy* (river bed, woods) or *soft* (snow) ground. Under these conditions, we argue that First Responders usually move from one place to another by means of one of the six motions shown in Figure 1. Since some of the motions differ one another only in terms of gait frequency, we run a series of experiments to estimate their natural gait frequency. For each motion, we tuned the number of beats per minute (bpm) of a metronome, until we found one representative of the volunteer movements. The values that we have found are reported in Table I. One beat corresponds to one foot, knee or elbow hit according to the considered motion.

To further extend the dataset, we have selected two testing paths: one without turns (straight line) and one with alternated left and right turns with different angles (zig-zag).

While a foot placement is the most common choice for HO systems, there is no known suitable placement for the detection of crawling and slithering motions. By referring to commonly considered placements for fitness-oriented devices and Human Activity Recognition systems [12], we decided to include waist, wrist and chest placement in the analysis.

TABLE I

AVERAGE GAIT FREQUENCY FOR THE 6 MOTIONS OF HOOD.

Motion	**Gait frequency (bpm)**
Slow walk	50
Normal walk	100
Run	150
Slow crawl	40
Fast crawl	80
Slither	36

III. Step Detection Procedure

As previously stated, the accuracy of Human Odometry systems heavily depends on the accuracy of the step detection procedure, i.e., on the ability of the HO system of identifying and keeping track of the number of taken steps. In addition to being mandatory for the estimation of the travelled distance, for example, the detection of steps is at the core of strategies such as Zero Velocity Update, that rely on the correct identification of all moments of contact between the foot and the ground to reduce the heading estimation drift.

Step detection procedures analyse the accelerations generated by the motion to identify each *step* taken by the person, implicitly assuming that there is a periodic pattern in the signal. While this assumption is trivial for walking activities, it becomes non-negligible for less common motions such as crawling and slithering; similarly while state-of-the-art step detection algorithms are designed to achieve good performance on even ground [4], other environments have been given significantly less attention. Lastly, while a foot placement is a natural choice for the analysis of vertical-stance activities, it is less straightforward to identify a suitable sensor placement for horizontal-stance activities.

As an example, Figure 4 reports, for each motion in HOOD dataset, the acceleration patterns a_x, a_y and a_z corresponding to the four sensor placements, generated by the person moving along a straight line path on a grass field. A simple observation of the patterns allows to draw the following conclusions.

- All motions generate a periodic acceleration pattern along at least one axis, for at least one sensor placement. In other words, the underlying assumption of human odometry algorithms holds valid for all HOOD motions.
- For some placements, vertical-stance motions produce clean periodic patterns along more than one axis (as an example, consider the chest placement for *run*). In such cases, merging the information coming from different axes may increase the step recognition accuracy.

To allow for meaningful comparisons between all the considered situations and provide a standard reference (i.e., unbiased to any specific motion or environment) for any other step detection procedure, we decided to apply in all cases a well-known, simple technique. We first filtered both the raw acceleration signals a_x, a_y and a_z and the raw angular velocity signals ω_x, ω_y and ω_z with a $6th$ order Butterworth low-pass filter (cut-off frequency of $5Hz$) to

Preprint submitted to 2015 IEEE/RSJ International Conference on Intelligent Robots and Systems. Received March 4, 2015.

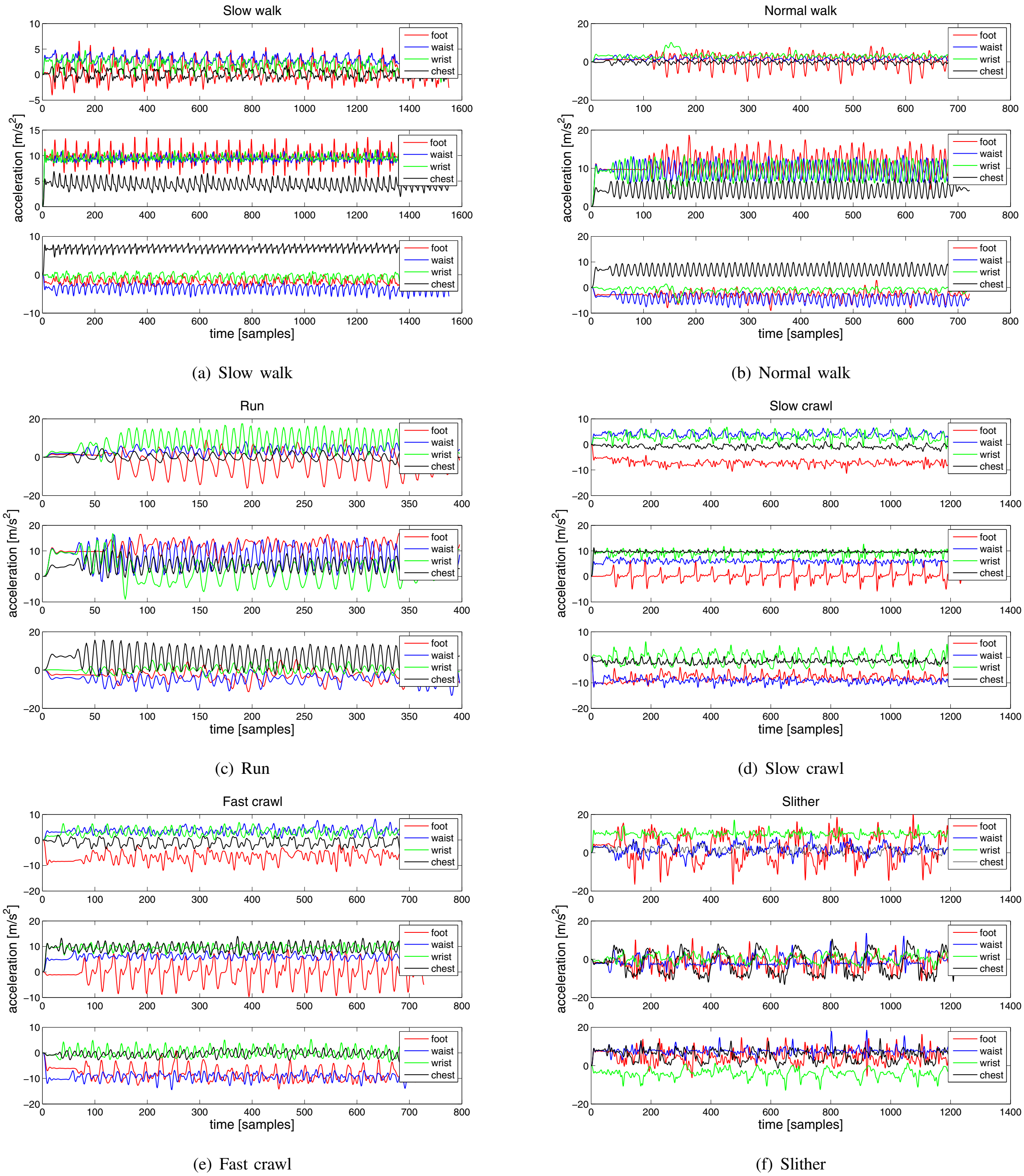

Fig. 4. Accelerometer values registered during the execution of *straight line* paths, for the 4 different device placements. For each motion, the graphs report the acceleration pattern a_x, a_y and a_z respectively, from top to bottom. All motions show a periodic pattern along at least one axis.

Preprint submitted to 2015 IEEE/RSJ International Conference on Intelligent Robots and Systems. Received March 4, 2015.

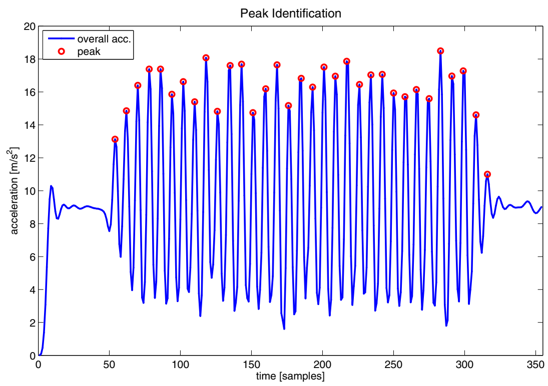

Fig. 5. The output of the step identification algorithm for the signal ov_a, referring to a person running along a zig-zag path on the snow, with the sensor placed at the chest: each peak (red dot) corresponds to one foot hit.

remove higher frequencies components, then we used a standard signal analysis algorithm[2] to identify the peaks. Given the considerations about merging axes to increase peak identification accuracy, we also extracted the number of peaks identified along the overall acceleration and the overall angular velocity signals, computed as, respectively:

$$ov_{a,i} = \sqrt{a_{x,i}^2 + a_{y,i}^2 + a_{z,i}^2}, \quad (1)$$

$$ov_{\omega,i} = \sqrt{\omega_{x,i}^2 + \omega_{y,i}^2 + \omega_{z,i}^2}, \quad (2)$$

where $a_{x,i}$ corresponds to the filtered acceleration value read on axis x at time instant i and $g_{y,i}$ corresponds to the filtered angular velocity value read on axis y at time instant i. For example, Figure 5 shows the output of the peak identification algorithm, when applied on the ov_a signal extracted from the recording of the volunteer running along a zig-zag path on the snow, with the sensor placed at the chest: one peak corresponds to one foot (knee or elbow hit for the crawling and slithering motions), and a pair of subsequent peaks corresponds to one step.

IV. Step Detection Accuracy across Environment Types

Tables II, III and IV analyze the step detection accuracy for the motions *slow walk*, *normal walk* and *run*, respectively, across the considered environments and sensor placements. Each table is divided in four parts, corresponding to the four considered placements. In each sub-table, the rows list the six environments of interest and the columns list the eight signals from which we estimate the number of steps, namely accelerations a_x, a_y, a_z, angular velocities $\omega_x, \omega_y, \omega_z$, overall acceleration ov_a, computed with (1), and overall angular velocity ov_ω, computed with (2). Each entry reports the mean relative error $E = E_{t,l,s}$ (percent) in the step count

[2]The peak identification procedure is available at: http://www.mathworks.com/matlabcentral/fileexchange/25500-peakfinder

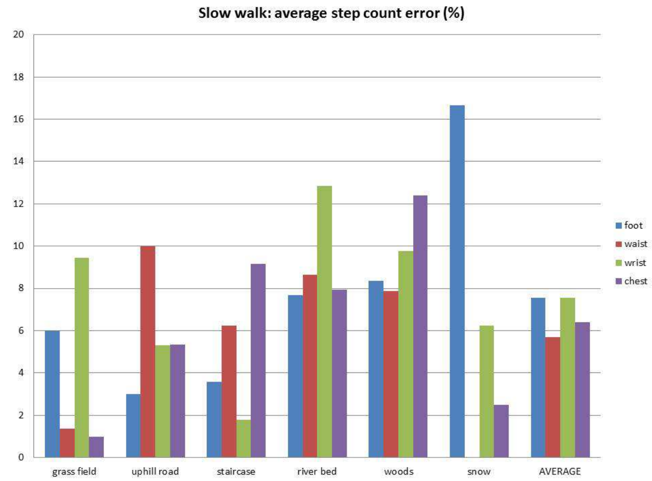

Fig. 6. Step counting minimum error for the *slow walk* motion across all considered environments and sensor placements.

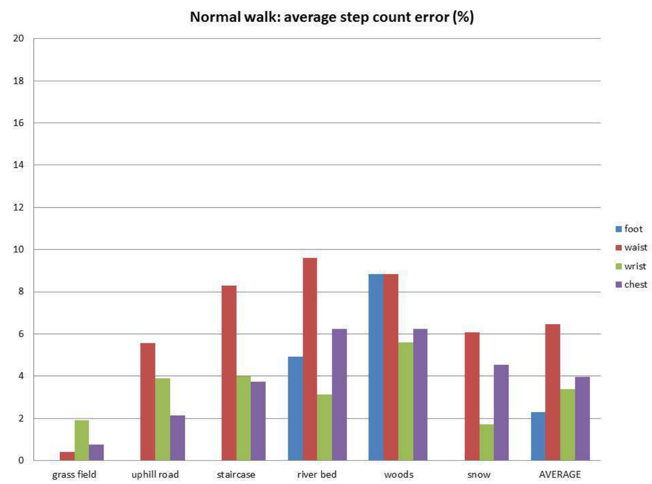

Fig. 7. Step counting minimum error for the *normal walk* motion across all considered environments and sensor placements.

corresponding to the given environment t, sensor location l and signal s, computed as:

$$E = \frac{(E_1 + E_2)}{2}. \quad (3)$$

Subscripts 1 and 2 define, respectively, straight and zig-zag paths. Each error E_n is computed as:

$$E_n = 100\frac{|S_n - S_n^\star|}{S_n}, \quad (4)$$

where S_n is the number of hits effectively performed by the volunteer in the considered trial and $S_n^\star$ is the estimated number of hits returned by the peak identification procedure.

A green cell filling marks the minimum error retrieved for each sensor placement and environment, i.e., the most accurate signal among $a_x, a_y, a_z, \omega_x, \omega_y, \omega_z, ov_a$ and ov_ω in each combination. Figures 6, 7 and 8 compare said minimum errors and allow drawing the following conclusions.

Regardless of the performed motion and considered sensor placement, the environment which allows for the highest

TABLE II

STEP COUNTING AVERAGE ERROR FOR THE SLOW WALK MOTION ACROSS ENVIRONMENT, SENSOR AXES AND PLACEMENT.

	Foot								Waist							
	ax	**ay**	**az**	**gx**	**gy**	**gz**	**ov_a**	**ov_g**	**ax**	**ay**	**az**	**gx**	**gy**	**gz**	**ov_a**	**ov_g**
Grass field	11,3	10,2	21,4	14,9	6	12	16,7	24,4	3,4	90,9	1,4	3,5	9,4	19	98,2	12,4
Uphill road	16.2	13.3	13.5	26.3	16.5	31.9	16.4	3	28.7	10	23	17	18.7	22.5	81.2	20.5
Staircase	15.7	21.5	19.1	3.6	27.3	30.3	20.3	13.8	22.6	9.4	6.3	12.8	19.2	17	8.3	12.2
River bed	16.9	16.9	17.9	19.6	23	9.2	7.7	20.3	48.9	19.4	9.6	16.4	8.7	23.1	92	33.6
Woods	20.5	21.6	8.4	17.9	21	26.5	23	22.2	21.4	7.9	20.2	15.6	15.8	19	34.8	22.5
Snow	20	25	20.8	23.3	16.7	16.7	20.8	20	11.1	15.7	0	22	5.1	9.6	15.7	23
	Wrist								**Chest**							
	ax	**ay**	**az**	**gx**	**gy**	**gz**	**ov_a**	**ov_g**	**ax**	**ay**	**az**	**gx**	**gy**	**gz**	**ov_a**	**ov_g**
Grass field	21,2	96,6	25	13,3	19,2	9,4	96,7	22,4	4	1	18,4	3,4	24,1	24,4	94	15,9
Uphill road	21.9	19.1	8.3	28.7	5.3	7	14.5	62	14.7	5.9	6.6	17.2	5.3	27.9	38.4	31.7
Staircase	18.7	22.7	1.8	19.1	4.6	4.8	20.7	65.9	20.3	9.1	17.8	9.1	22.7	11.6	24.1	18.7
River bed	26.4	15.3	19.4	13.2	12.8	16	38.2	53.5	58.9	7.9	10.6	8.1	23.8	15.8	74	21.1
Woods	9.8	23.9	16	10.5	12.1	12.7	13.9	40.1	32.9	42.7	34.2	38.2	25.4	29.3	51.5	12.4
Snow	16.7	20.1	16	12.5	6.3	30.6	23.6	17.4	40	7.1	2.5	17.9	6.8	14.6	42.1	56.4

TABLE III

STEP COUNTING AVERAGE ERROR FOR THE NORMAL WALK MOTION ACROSS ENVIRONMENT, SENSOR AXES AND PLACEMENT.

	Foot								Waist							
	ax	**ay**	**az**	**gx**	**gy**	**gz**	**ov_a**	**ov_g**	**ax**	**ay**	**az**	**gx**	**gy**	**gz**	**ov_a**	**ov_g**
Grass field	11,5	11,4	37,2	8,7	15,3	20,2	16,2	0	3,6	1,4	1,9	18,9	12,4	12,7	0,4	37,3
Uphill road	13.3	8.1	11.3	0	27.2	3.2	13.7	35.7	5.6	6.7	26.2	11.8	7.2	26.7	6	7.9
Staircase	23.5	0	11.1	2	25.3	20.7	16.1	4.8	19.8	8.3	17.7	20.5	19.8	12.1	14.2	33.6
River bed	12.5	11.8	4.9	12	21.2	19.8	13.4	18.8	29.2	25.8	9.6	17.5	13.1	24.2	29.2	16.8
Woods	28.2	21.5	16.3	11.3	21.2	16.5	24.6	8.8	19.9	14.4	25.8	28.1	8.8	28.4	17.9	14.8
Snow	0	23.3	14.2	0	9.2	7.1	11.3	13.3	24.3	19.3	6.1	13.6	21.8	8.6	16.8	12.1
	Wrist								**Chest**							
	ax	**ay**	**az**	**gx**	**gy**	**gz**	**ov_a**	**ov_g**	**ax**	**ay**	**az**	**gx**	**gy**	**gz**	**ov_a**	**ov_g**
Grass field	57,7	2,5	23,1	20,2	12,7	18,4	1,9	7,2	13,2	0,8	0,9	11,3	13,8	45,1	1,2	56,6
Uphill road	9.7	7.8	10.4	6.1	13	4.3	5.8	3.9	2.2	15	22.4	2.4	14.9	16.8	4.3	4.8
Staircase	25.3	15.1	16.1	12.7	4	7.6	27.5	20.1	20.9	10.6	23.8	33.7	17.2	3.7	26.3	28.3
River bed	29.4	50.7	23.8	5.8	3.1	5.8	29.4	13.6	19.4	11.3	7.3	7	19.4	6.3	20.9	16.7
Woods	12.9	26.4	15.8	11.2	5.6	21.4	11.8	23.6	9.6	11.1	43.4	12	26.1	9.1	11.1	6.3
Snow	20.6	15.4	1.7	6.3	28	25.7	17.7	13.2	11.7	4.5	12.3	7.9	7.9	11.2	14.5	16.7

TABLE IV

STEP COUNTING AVERAGE ERROR FOR THE RUN MOTION ACROSS ENVIRONMENT, SENSOR AXES AND PLACEMENT.

	Foot								Waist							
	ax	**ay**	**az**	**gx**	**gy**	**gz**	**ov_a**	**ov_g**	**ax**	**ay**	**az**	**gx**	**gy**	**gz**	**ov_a**	**ov_g**
Grass field	2,8	18,8	12,5	1,5	5,1	5,6	14,4	24	14,1	1	21,9	27,6	9,2	8,2	1,2	11,1
Uphill road	18.8	3.6	7.6	2.3	13.1	4.1	9.9	2.3	1.1	0	16.5	7.5	9.3	11.5	1.1	17.1
Staircase	3.7	5.6	11.1	1.9	14.8	11.1	13	8.3	2	1.8	6.6	16.5	11.4	30.3	2	9.6
River bed	14.1	2.6	27.7	23.5	27.2	7.3	5.8	6.8	0	7	10.6	45.6	21.6	20.5	1	15.8
Woods	12.3	6.6	4.9	11.2	19.2	6	6	11.8	3.6	16.1	25.7	10.4	18.9	33	2.5	13.4
Snow	18.3	9.1	14.7	7.1	5.6	9.1	11.1	6.4	4.2	6.7	1.7	16.7	21.7	16.7	4.2	10
	Wrist								**Chest**							
	ax	**ay**	**az**	**gx**	**gy**	**gz**	**ov_a**	**ov_g**	**ax**	**ay**	**az**	**gx**	**gy**	**gz**	**ov_a**	**ov_g**
Grass field	0,8	5,1	12,7	2	28,5	7,2	2	11,6	4,1	7,3	0,8	7,6	5,5	2,5	0,5	24,5
Uphill road	24.3	7	7.5	21.4	4.2	4.2	3	26.3	2.8	4.2	28.5	2.8	26.7	12.5	1.4	11.8
Staircase	27	17.3	7.2	35.2	27.9	17.3	1.8	27	1.9	2.9	2.8	6.5	25.6	8.5	1.9	15
River bed	24.6	17.4	7.7	27.5	16.5	2	2	18.4	1	7.5	16.3	5.4	20	10.8	2.7	13.1
Woods	12.2	9	23.4	7.9	2.2	12.7	7.7	13.5	0	3.1	12.3	23.1	41.6	2	0	9.4
Snow	6.5	2.1	18.9	11.3	4.2	3	0	14.2	1.6	3.1	22.3	4.5	21.4	3.1	1.6	20.2

Preprint submitted to 2015 IEEE/RSJ International Conference
on Intelligent Robots and Systems. Received March 4, 2015.

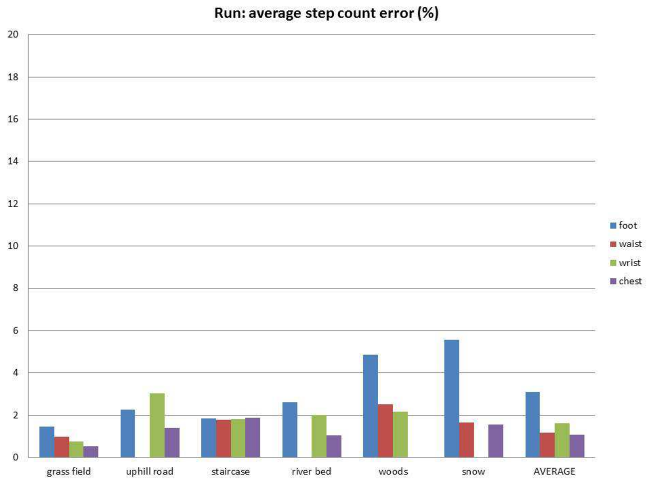

Fig. 8. Step counting minimum error for the *run* motion across all considered environments and sensor placements.

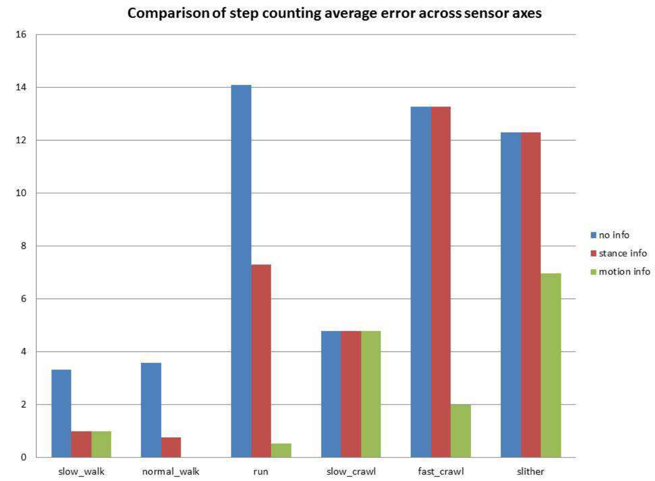

Fig. 9. Minimum step counting average errors assuming no specific knowledge (blue line), information about the person stance (red line) and exact knowledge of the motion to be performed (green line).

accuracy in the step detection is, unsurprisingly, the grass field, i.e., a flat, even ground. Conversely, the environment which poses the biggest challenges to the Human Odometry system is the woods, i.e., a sloping, rocky ground. The analysis points out that while the slope has a minor effect on the accuracy of the step detection, the evenness of the ground is crucial, since it affects both the regularity and the heaviness of the steps, which are two parameters on which the step detection algorithm relies for an accurate recognition. As a further proof of this fact, experiments prove that accuracy generally increases with the pace of the motion, which is proportional to the heaviness of the step (for all environments, errors are higher when the person is walking slowly and lower when the person is running).

An analysis of the step detection accuracy across the different environments allows noting that a chest placement provides the highest overall accuracy (error of 3.80% averaged over all environments), with no significant gain over the other placements (the highest error, registered for a wrist placement, is 4.44%). Lastly, it is important to notice that the ground conditions seem to have a lesser impact on the step detection accuracy than the performed motion. For example, Figure 8 shows that the best sensor placement to detect a person running is the torso (chest or waist), regardless of the environment in which the activity takes place.

V. Step Detection Accuracy across Motion Types

Table V considers the grass field exclusively, to analyse the dependency of the step detection accuracy on the performed motion. The table is divided in four parts, corresponding to the considered placements. In each sub-table, the rows list the six motions of interest and the columns list the eight signals from which we estimate the number of steps. Each entry in the table reports the mean relative error $E = E_{m,l,s}$ (percent) in the step count corresponding to the given motion m, sensor location l and signal s, computed as:

$$E = \frac{(E_1 + E_2)}{2}, \tag{5}$$

where subscripts 1 and 2 define, again, straight and zig-zag paths and each error E_n is computed with (4).

Table V allows to draw the following conclusions.

In case no information is given about the types of motion of interest, i.e., we aim at minimizing the average error across all the motions, the best signal to consider is a_x of a waist-placed sensor (error: 8.56% avg, 3.33% min, 14.08% max). This finding supports the intuition that the waist, being the closest location to the center of mass of the person, is subject to similar accelerations during all the motions.

If we focus exclusively on vertical-stance activities, or if we can detect the stance of the person and appropriately control the human odometry system, the best signal to consider is a_y of a chest-placed sensor (error: 3.02% avg, 0.76% min, 7.30% max), which confirms the findings of the environment-dependency analysis reported in Section 2. Unlike foot placement, a chest placement generates signals which are not heavily affected by the gait frequency (Figure 4), thus allowing for the use of a single, generalized peak identification algorithm. Conversely, if we focus exclusively on horizontal-stance activities, the best signal to consider is again a_x of a waist-placed sensor (error: 10.13% avg, 4.80% min, 13.28% max). The reduced accuracy, for a placement close to the center of mass, confirms that horizontal-stance motions generate particularly noisy signals patterns, which are harder to analyse. Finally, if we knew at all times which motion the person were going to perform, we could consistently minimize the error for that motion exclusively.

In particular:

- the best signal to monitor a *slow walk* is a_y of a chest-placed sensor (error: 0.99% avg, 0% min, 1.60% max);
- the signal that minimizes the error for the *normal walk* motion is ov_g of a foot-placed sensor (error: 0% avg);
- signal ov_a of a chest-placed sensor is the best for the *run* motion, (error: 0.52% avg, 0% min, 1.56% max);
- g_x of a wrist-placed sensor is best suited for *slow crawl*

TABLE V

STEP COUNTING AVERAGE ERROR ACROSS SENSORS, AXES AND PLACEMENTS.

	Foot								Waist							
	ax	**ay**	**az**	**gx**	**gy**	**gz**	**ov_a**	**ov_g**	**ax**	**ay**	**az**	**gx**	**gy**	**gz**	**ov_a**	**ov_g**
Slow walk	11,3	10,2	21,4	14,9	6	12	16,7	24,4	3,4	90,9	1,4	3,5	9,4	19	98,2	12,4
Normal walk	11,5	11,4	37,2	8,7	15,3	20,2	16,2	0	3,6	1,4	1,9	18,9	12,4	12,7	0,4	37,3
Run	2,8	18,8	12,5	1,5	5,1	5,6	14,4	24	14,1	1	21,9	27,6	9,2	8,2	1,2	11,1
Slow crawl	16	5	13,7	31,5	16,3	22	34,2	24	4,8	15	46,8	22,5	7,9	22,3	91,7	9,2
Fast crawl	22,1	5,4	4,8	13,6	20,3	20,2	13,1	17,1	13,3	30,5	11,2	13	22,6	15,6	7,4	20,4
Slither	34,3	64,2	72,5	28,7	52,6	42,8	129,1	112	12,3	14,6	13,6	9,3	44,3	26,5	19,5	33
	Wrist								**Chest**							
	ax	**ay**	**az**	**gx**	**gy**	**gz**	**ov_a**	**ov_g**	**ax**	**ay**	**az**	**gx**	**gy**	**gz**	**ov_a**	**ov_g**
Slow walk	21,2	96,6	25	13,3	19,2	9,4	96,7	22,4	4	1	18,4	3,4	24,1	24,4	94	15,9
Normal walk	57,7	2,5	23,1	20,2	12,7	18,4	1,92	7,2	13,2	0,8	0,9	11,3	13,8	45,1	1,2	56,6
Run	0,8	5,1	12,7	2	28,5	7,2	2	11,6	4,1	7,3	0,8	7,6	5,5	2,5	0,5	24,5
Slow crawl	15,6	23,1	24,9	4,8	33,2	43,2	35,7	12,6	22,6	96	15,3	6,6	12	11,4	96	13,9
Fast crawl	12,3	9,3	2	2,9	20,9	4,8	23,1	7	3,1	41	2,4	22,9	17,5	19,5	18,5	19,2
Slither	9,5	11,1	7	31,2	49,4	67,3	21,2	30,6	27	25,2	20,6	9,5	46,7	24,2	17,5	14,5

motions (error: 4.79% avg, 3.57% min, 6.25% max);

- the best signal for *fast crawl* is a_z of a wrist-placed sensor (error: 1.99% avg, 1.43% min, 2.46% max);
- the signal to analyse for *slither* is a_z of a wrist-placed sensor (error: 6.96% avg, 4.17% min, 14.70% max);

Figure 9 shows the average errors that we can obtain by adding information about the stance of the person or the particular motion to be performed.

VI. CONCLUSIONS

We present the Human Odometry Outdoor Data Set (HOOD), a public collection of labelled accelerometer and gyroscope data recordings to be used for the design and validation of Human Odometry systems. We compare four different sensor placements (foot, waist, wrist, chest) to identify the most suitable one for different types of motions (ranging from walking to crawling) and ground conditions (grass field, uphill road, staircase, river bed, woods, snow). We analyse the performance of a simple step detection algorithm to extract useful information about the incidence of motion and environment on the step detection accuracy and to determine the most suitable sensor placement with respect to the different motions and conditions.

REFERENCES

[1] B. Doroodgar, M. Ficocelli, B. Mobedi, and G. Nejat, "The search for survivors: Cooperative human-robot interaction in search and rescue environments using semi-autonomous robots," in *Proceedings of the 2010 IEEE International Conference on Robotics and Automation (ICRA 2010)*, Anchorage, Alaska, USA, May 2010.

[2] C. Randell, C. Djiallis, and H. Muller, "Personal position measurement using dead reckoning," in *Proceedings of the 2003 IEEE International Symposium on Wearable Computers (ISWC 2003)*, October 2003.

[3] S. Beauregard and H. Haas, "Pedestrian dead reckoning: A basis for personal positioning," in *Proceedings of the 2006 Workshop on Positioning, Navigation and Communication (WPNC 2006)*, March 2006.

[4] A. J. Ruiz, F. Granja, J. P. Honorato, and J. Rosas, "Accurate pedestrian indoor navigation by tightly coupling foot-mounted IMU and RFID measurements," *IEEE Transactions on Instrumentation and Measurement*, vol. 61, no. 1, pp. 178–189, 2012.

[5] J. Collin, O. Mezentsev, and G. Lachapelle, "Indoor positioning system using accelerometry and high accuracy heading sensors," in *Proceedings of the 2003 ION Conference on GPS/GNSS (GPS/GNSS 2003)*, Portland, OR, USA, September 2003.

[6] L. Ojeda and J. Borenstein, "Non-GPS navigation for security personnel and first responders," *Journal of Navigation*, vol. 60, no. 3, pp. 391–407, 2007.

[7] J. Rantakokko, J. Rydell, P. Stromback, P. Handel, J. Callmer, D. Tornqvist, F. Gustafsson, M. Jobs, and M. Gruden, "Accurate and reliable soldier and first responder indoor positioning: multisensor systems and cooperative localization," *IEEE Wireless Communications*, vol. 18, no. 2, pp. 10–18, 2011.

[8] E. P. Herrera, H. Kaufmann, J. Secue, R. Quiros, and G. Fabregat, "Improving data fusion in personal positioning systems for outdoor environments," *Information Fusion*, vol. 14, no. 1, pp. 45–56, 2013.

[9] J. Aggarwal and M. Ryoo, "Human activity analysis: a review," *ACM Computing Surveys*, vol. 43, no. 3, 2011.

[10] O. Perrin, P. Terrier, Q. Ladetto, B. Merminod, and Y. Schutz, "Improvement of walking speed prediction by accelerometry and altimetry, validated by satellite positioning," *Medical and Biological Engineering and Computing*, vol. 38, no. 2, pp. 164–168, 2000.

[11] M. Attia, A. Moussa, and N. El-Sheimy, "Map aided pedestrian dead reckoning using buildings information for indoor navigation applications," *Positioning*, vol. 4, pp. 227–239, 2013.

[12] D. Olguin and A. Pentland, "Human activity recognition: accuracy across common locations for wearable sensors," in *Proceedings of the 2006 IEEE International Symposium on Wearable Computers (ISWC 2006)*, Montreaux, Switzerland, October 2006.

Preprint submitted to 2015 IEEE/RSJ International Conference
on Intelligent Robots and Systems. Received March 4, 2015.